

YOUNG LUNAR VOLCANISM: IRREGULAR MARE PATCHES AS DRAINED LAVA PONDS AND INFLATED FLOWS. J. D. Stopar¹, M. S. Robinson², C. H. van der Bogert³, H. Hiesinger³, L. R. Ostrach⁴, T. A. Giguere⁵, and S. J. Lawrence⁶, ¹Lunar and Planetary Institute, USRA, Houston, TX. ²Arizona State University. ³University of Münster, Germany. ⁴USGS, Flagstaff, AZ. ⁵University of Hawaii. ⁶NASA Johnson Space Center, Houston, TX.

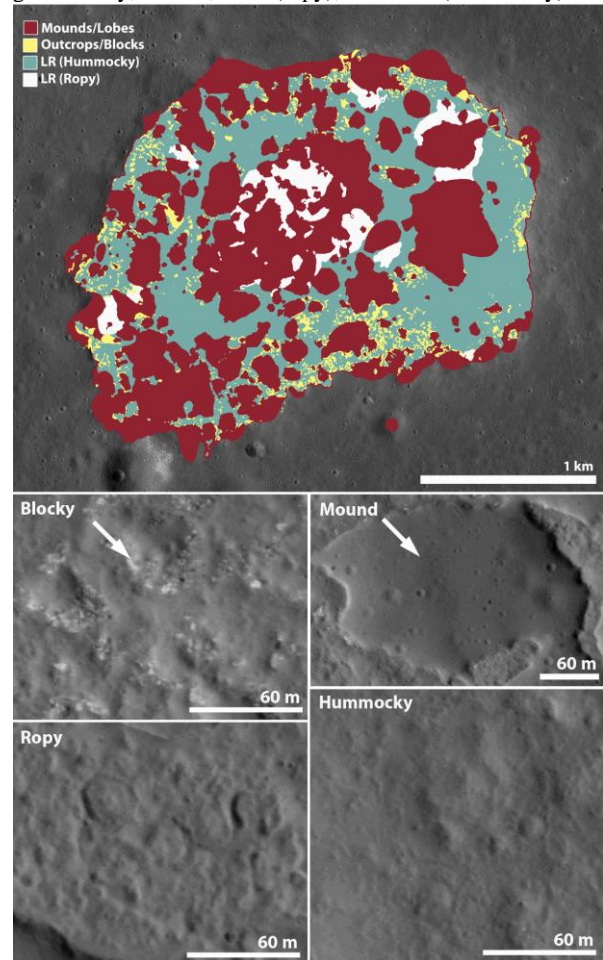
Introduction: Irregular mare patches (IMPs) were previously proposed as sites of young lunar volcanism and/or endogenic activity [1-3], raising the possibility that volcanism on the Moon may not have ended ~1 Ga as determined from surface ages [4]. The widespread occurrence of more than 70 IMPs on the lunar nearside suggests a correlation with Th-rich PKT regions and a basaltic composition [1,2].

IMPs exhibit at least two types of deposit morphologies: (a) dome-like, steep-sided and smooth mounds and (b) low-relief ropy (LRR) to hummocky (LRH) materials (**Fig. 1**). Morphologic indicators such as steep (>40°) margin slopes across distances <10 m and crisp boundaries imply ages less than a few 100 Ma [e.g., 1-3]. The IMPs also have relatively few superposed craters >10 m in diameter, and young absolute model ages, which when combined with their superposition on young crater deposits like the continuous ejecta of Aristarchus crater, imply ages ~10 Ma to 100 Ma [1,2]. However, the mounds do not exhibit blocky crater morphologies, nor fracturing typical of young volcanic deposits, and the mound texture resembles that of mature regolith [e.g., 2,5], implying a much older age (~3.5 Ga). These contrasting indicators have led to the proposal of widely varying formation mechanisms that range from ancient volcanism modified by recent tectonism [6] or outgassing [3,7], ancient volcanism of atypical materials [8], to Copernican-era volcanism [1,2].

Study Objectives: Here, we investigate IMP formation by re-examining the range of IMP morphologies using high-resolution LROC NAC-derived topography and stratigraphies for 15 IMPs, including the largest individual examples: Ina, Sosigenes, Maskelyne, Nubium, Cauchy, as well as some smaller examples in Mare Tranquilitatis and near Manilus, Carrel, Hyginus, Tobias Meyer, Gruithuisen, Aristarchus, and Arago craters.

Study Interpretations: Based primarily on the presence of moats, inflation pits, and break-out morphologies [5,9], as well as crisp margins [e.g., 1,2,5,9] and stratigraphic relationships [1-3], we continue to interpret the IMPs as young landforms composed primarily of inflated lava flows (**Fig. 2**). Flow inflation associated with eruptions from multiple sources (single eruptive events with several vents, or as a sequence of eruptions) is most consistent with the overall morphologies and stratigraphies of the studied IMPs.

Fig. 1 Geomorphologic map of the Ina IMP (5.30°E, 18.65°N). High-resolution examples of deposit morphologies: blocky, mound, LRR (ropy), and LRH (hummocky).



However, the meter-scale or larger fractures anticipated with young basaltic lava flows, ponds, and squeeze-ups are lacking within the mounds [5], suggesting different physical characteristics for the mounds. Block-less craters on the mounds suggest at least 5 m of friable or poorly cohesive materials, yet the mound margins exhibit steep slopes requiring significant material strength. Blocks are not common on the mounds [e.g., 6,10] but are sometimes excavated by impacts. Pyroclastic materials [11], late-stage “foamy lavas” [8], and/or rubble-style flows with blocks <30 cm in dimension could potentially resolve this inconsistency. Alternatively, smaller-scale fractures (e.g., <30 cm in length) on mound surfaces may have been eroded in the last 10-100 Myr [e.g., 12-13].

Because of the similarities in albedo, texture, and composition between mounds and surrounding mare deposits, some mounds might be composed of rafted debris (e.g., regolith, lava plates) and/or pyroclastic materials that have been caught up in the flows [e.g., 20]. Profiles of mounds near the rims (along the interior walls) of the IMPs can be interpreted as either slumped materials or in-situ extrusions. Regolith and/or pyroclastic “rafts” are potentially consistent with optical and spectral observations suggesting that IMP mounds have similar physical properties to, but are also less mature than, surrounding maria [1-3,14-17].

Our current preferred interpretation for the studied IMPs are drained lava ponds, where the current surface deposits are the last residual materials to be emplaced. The absence of an equipotential surface at most IMPs makes it unlikely that they represent solidified lava ponds without drainage. At each of the IMPs, LRR, LRH, and mounds have morphologies and slopes (and no evidence for faulting or fracturing) that suggest emplacement on a sloping surface nearly the same as the present topography, and thus are either coeval with, or post-date, any formative collapse.

Several previous workers have proposed that the mounds represent squeeze-ups of residual lava extruded during magma withdrawal and fragmentation of a solid lava lake surface (where the mounds are the youngest deposits) [1-2,8-9]. Based on our detailed re-examination, the mounds and the LRR and LRH deposits are highly interconnected, and likely represent different parts of the same flow series [e.g., 5], either as eruptions, breakouts, and/or squeeze-ups (**Fig. 2**).

The LRR and LRH deposits and mounds might be a relatively thin series of flows draping prior accumulations of collapsed and brecciated lava and debris, as suggested by outcrops of blocky material at the bases of some of the LRR, LRH, and mound deposits (**Fig. 2**). Blocky deposits are primarily located around the perimeters of the IMPs’ interiors, where fracturing may be most intense in a collapsed lava pond/lake [e.g., 9], or where flows were thinner due to downslope drainage (**Figs. 1, 2**). Alternatively, some of blocky deposits may represent a lower portion of the flow with different physical characteristics (e.g., in density or vesicle content).

As volcanic flux waned, lava in the IMPs drained to the lowest points [e.g., 5], where it may have briefly ponded and/or inflated. Both the mounds and LRH flows experienced inflation as a result of few degree slopes and topography (and obstacles like other mounds or pre-existing craters), flow rate, and rheology [e.g., 1,5] (**Fig. 2**). Some of the subdued craters on the mounds (**Fig. 1**) were previously suggested to be summit craters or degraded impact craters [e.g., 3,5,9].

Alternatively, they could be deflation pits caused by downslope breakouts of molten material from within the inflated lobe. Many of the mounds are asymmetric in the downslope direction, and some appear to have coalesced into larger mounds or filled in pre-existing craters and/or sags in a semi-molten pond [e.g., 5,9].

Summary: IMPs most likely represent the final residual materials associated with a drained lava pond or lake. Flow textures, inflation, and deposit morphologies were controlled by lava density (and gas/vesicle content), flux, viscosity, and topography. Even though physical properties of various volcanic materials could affect crater scaling and retention [e.g., 18-19], based on stratigraphic relationships and crisp morphologies, the volcanism associated with the IMPs mostly likely occurred in the last few 100 myr.

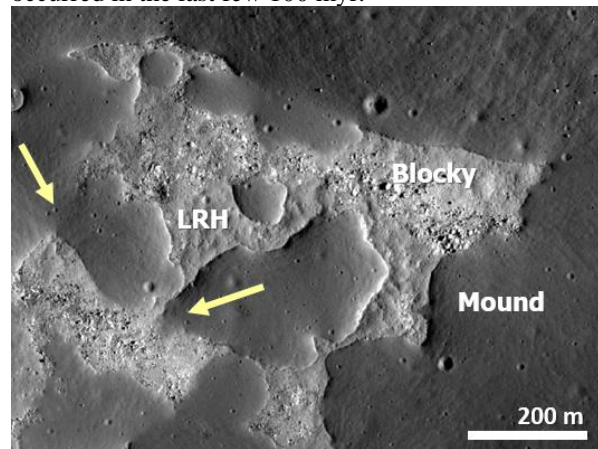


Fig. 2. Lobate deposits interpreted as breakout flows or squeeze-ups (arrows) in the Sosigenes IMP (19.07°E, 8.33°N). LRH materials interpreted as partly inflated flows.

Acknowledgements: This work was funded by the Lunar Reconnaissance Orbiter Camera and Lunar Reconnaissance Orbiter project.

References: [1] Braden et al. (2014) *Nat. Geosci.*, 10.1038/ngeo2252. [2] Braden (2013) PhD Arizona State University, UMI #3605207. [3] Schultz et al. (2006) *Nature*, 10.1038/nature05303. [4] Hiesinger et al. (2011) *GSA Special Paper 477*, p.1-51. [5] Garry et al. (2012) *JGR*, 10.1029/2011JE003981. [6] Qiao et al. (2016) *LPSC #2002*. [7] Stooke (2012) *LPSC 1011*. [8] Head et al. (2016) *Ann. Meeting LEAG #5069*. [9] Strain and El-Baz (1980) *Proc. 11th LPSC: 2437-2446*. [10] Elder et al. (2016) *LPSC #2785*. [11] Carter et al. (2013) *LPSC #2146*. [12] Speyerer et al. (2016) 10.1038/nature19829. [13] Fassett and Thomson (2014) *JGR*, 10.1002/2014JE004698. [14] Bennett et al. (2015) *LPSC #2646*. [15] Staid et al. (2011) *LPSC #2499*. [16] Donaldson-Hanna et al. (2016) *LPSC #2127*. [17] Grice et al. (2016) *LPSC #2106*. [18] Dundas et al. (2010) *GRL*, 10.1029/2010GL042869. [19] van der Bogert et al. (2017) 10.1016/j.icarus.2016.11.040. [20] Richter and Murata (1966) *USGS Prof. Paper 537*.